Journal of Photochemistry and Photobiology A: Chemistry 221 (2011) 199–203

Contents lists available at ScienceDirect

Journal of Photochemistry and Photobiology A: Chemistry

journal homepage: www.elsevier.com/locate/jphotochem

Surface-enhanced Raman scattering on multilayered nanodot arrays obtained using anodic porous alumina mask

Toshiaki Kondo[b], Hayato Miyazaki[a], Kazuyuki Nishio[a,b], Hideki Masuda[a,b,*]

[a] Department of Applied Chemistry, Tokyo Metropolitan University, 1-1 Minamiosawa, Hachioji, Tokyo 192-0397, Japan
[b] Kanagawa Academy of Science and Technology (KAST), 5-4-30 Nishihashimoto, Sagamihara, Kanagawa 252-0131, Japan

ARTICLE INFO

Article history:
Available online 13 April 2011

Keywords:
Anodic porous alumina
Plasmon
SERS
Three-dimensional structure

ABSTRACT

The fabrication of 3D multilayered nanodot arrays composed of metal (Au) and dielectric material (Al_2O_3) using ordered anodic porous alumina as a mask for vacuum evaporation was demonstrated. The obtained ordered multilayered dot arrays produced the accumulated nanogaps with controlled sizes, which can effectively enhance the electric field of incident light. The obtained structures with multilayered nanodots could be applied to the substrate for surface-enhanced Raman scattering (SERS) measurement, and larger SERS signals were obtained at larger numbers of multilayers and smaller gap seizes, corresponding to the effective enhancement of the electric field of incident light.

1. Introduction

The fabrication of two-dimensional (2D) and three-dimensional (3D) ordered arrays of metal nanostructures has attracted increasing attention owing to their capability to enhance the electric field of incident light based on localized surface plasmon (LSP) [1–6]. Various types of applications of 2D and 3D metal structures based on LSP, such as sensing devices or nonlinear optical devices, have been proposed [7–9]. Among them, the fabrication of plasmonic devices with nanogaps, which exist between two metal particles, is effective for enhancing the electric field of incident light. To optimize the degree of enhancement of the electric field of incident light, control of the geometrical structures of the nanogaps between metal nanoparticles is essential. A multilayered structure composed of metal and dielectric materials has been proposed as a candidate for the structures, which can produce the accumulated nanogaps [10] or nanoslits [11] with controlled sizes. The small gaps or slits formed in the multilayer of metal and dielectric material are effective for the enhancement of the electric field of incident light. Usually, the multilayered structure composed of metal and dielectric material is fabricated by electron beam lithographic technique. Although this technique allows the fabrication of multilayered structures of metal and dielectric material with desired shapes, the fabrication requires a long time and, thus, it is difficult to form samples with a large sample area at a low cost.

In previous reports, we have shown the fabrication of 2D metal (Au, Ag) nanodot arrays using anodic porous alumina as a mask for vacuum deposition, and have shown the applicability of the obtained 2D metal dot array to plasmonic devices [12–17]. Anodic porous alumina, which is formed by anodization of Al in acidic electrolyte, is a typical self-ordered porous material composed of uniform-sized straight pores perpendicular to the surface [18]. One of the advantageous points of this process is that the size and shape of the obtained metal dot can be controlled by changing the geometrical structures of the porous alumina used as a mask. In addition, large sized samples with metal nanodots could be obtained without any expensive apparatus. In the present report, we demonstrate the fabrication of a multilayered nanodot array, which produces accumulated nanogaps between metal and dielectric materials, using an anodic porous alumina mask, and its application to the substrate for surface-enhanced Raman scattering (SERS) measurements based on its capability to effectively enhance the electric field of incident light. In this process, multilayered structures composed of metal (Au) and dielectric materials (Al_2O_3) were formed by alternative vacuum deposition using a porous alumina mask. Fabrication of this type of nanodot arrays is the first example of the multilayered nanostructures prepared by anodic porous alumina mask. The process of preparing the multilayered metal/dielectric materials is simple and easy and allows the formation of large sized samples with large numbers of accumulated nanogaps with controlled sizes, which is effective for the enhancement of the electric field of incident light.

* Corresponding author at: Department of Applied Chemistry, Tokyo Metropolitan University, 1-1 Minamiosawa, Hachioji, Tokyo 192-0397, Japan.
Tel.: +81 42 677 2843; fax: +81 42 677 2841.
E-mail addresses: masuda-hideki@c.metro-u.ac.jp, masuda-hideki@tmu.ac.jp (H. Masuda).

1010-6030/$ – see front matter © 2011 Elsevier B.V. All rights reserved.
doi:10.1016/j.jphotochem.2011.03.019

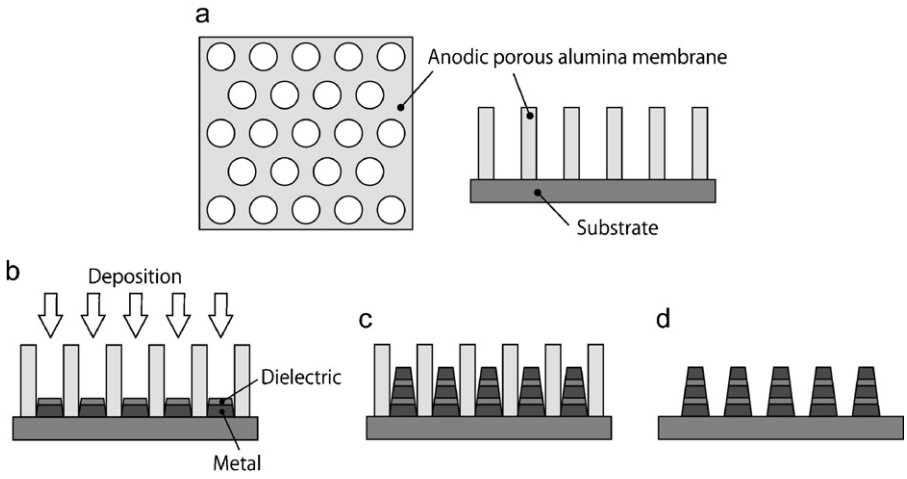

Fig. 1. Fabrication for multilayered nanodot using anodic porous alumina membrane. (a) An anodic porous alumina membrane is set on the substrate. (b) Metal and dielectric materials are alternately deposited by electron beam sputtering. (c) Multilayered structures are formed in each nanohole of the porous alumina membrane. (d) By removing the membrane of (c), multilayered nanodots are obtained.

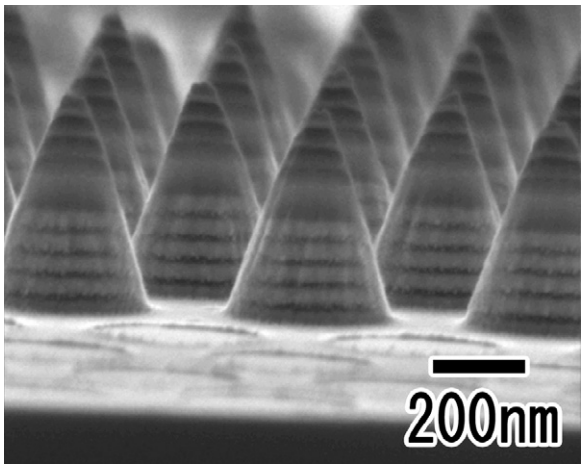

Fig. 2. SEM image of multilayered nanodot array. The number of Au layers was 10. The thicknesses of the Au and Al_2O_3 layers were 30 and 10 nm, respectively.

2. Experimental

A multilayered nanodot composed of Au and Al_2O_3 was obtained using anodic porous alumina membranes as evaporation masks. Fig. 1 shows the schematic for the preparation of multilayered nanodots. The process for the preparation of alumina masks was similar to that reported previously [12–17]. The porous alumina with 500 and 100 nm hole intervals was used as a mask. For the preparation of porous alumina with a 500 nm interval, an Al plate was anodized in 0.1 M phosphoric acid solution at a constant voltage of 195 V for 8 min. The porous alumina with a 100 nm hole interval was prepared by anodization in 0.5 M oxalic acid at 40 V using two step anodization. In the case of the porous alumina with hole interval of 500 nm, the Al was pretextured by imprinting using a mold with an ordered array of convexities to generate an ideally ordered hole arrangement in anodic porous alumina prior to anodization. Porous alumina masks with through holes were obtained by the selective dissolution of Al in saturated I_2 methanol solution followed by the removal of the bottom part of the porous alumina films by using an ion milling apparatus. The thickness of the alumina membrane was usually approximately 1 μm. The hole sizes of the alumina mask were adjusted by postetching treatment in 5 wt% phosphoric acid solution. The porous alumina masks were set up on the glass substrate. Au and Al_2O_3 were deposited alternately onto the substrate through the nanoholes of the alumina mask using an electron-beam sputtering apparatus. The thicknesses of the Au and alumina layers were controlled using a film thickness monitor. After the deposition, the multilayered nanodot array on the substrate was obtained by removing the alumina mask mechanically. The multilayered nanodot array was observed by using a field emission scanning electron microscope (FE-SEM; JEOL).

The degree of enhancement of the electric field of incident light at the multilayered nanodot was calculated by 3D finite-difference

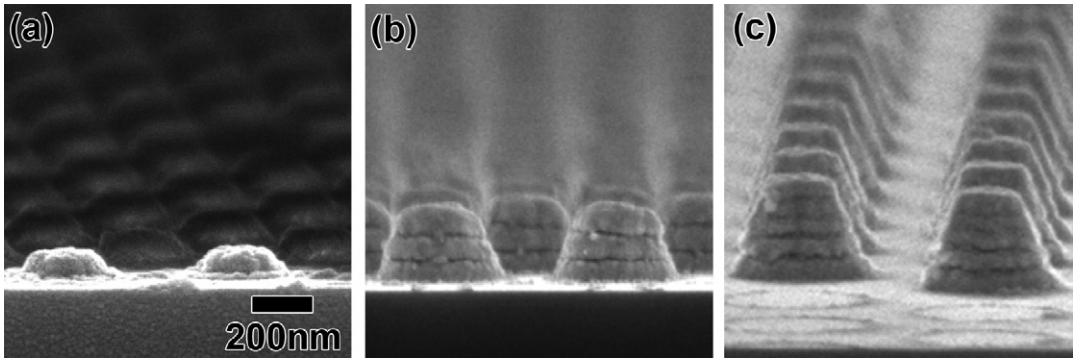

Fig. 3. SEM images of multilayered nanodot with different numbers of Au layers. The numbers of Au layers were (a) 1, (b) 3, and (c) 5.

time-domain (FDTD) method using a commercially available software (Crystalwave; Photon Design Inc.). The calculation was carried out under condition of the continuous incident light of 633 nm. The grid size for the calculation field was 1–2 nm, and the boundary condition of the calculation area was periodic.

Raman scattering spectra of pyridine molecules were obtained using a Raman scattering spectrometer (NRS-3100; JASCO) equipped with a He–Ne laser (633 nm) as a light source. The size of the laser spot was 13 μm. The laser power was 0.9 μW. The duration of irradiation and accumulation of signals were 3 s and 10 times, respectively. The substrate with the nanodot arrays was dipped in a pyridine solution (HPLC grade, >99.9%) and dried in air before the measurement.

3. Results and discussion

Fig. 2 shows the SEM image of the typical multilayered nanodots composed of Au and Al_2O_3 prepared by the present process. The number of layers was 19, 10 layers of which were composed of Au layers. The top layer of multilayered nanodots was Au. From Fig. 3, it can be confirmed that uniform-sized multilayered nanodots can be formed on the glass substrate. The straight high-aspect-ratio holes in the porous alumina mask allowed the formation of multilayered dots with high aspect feature. The shape of each dot is circular conical, reflecting the shadowing effect accompanied by the decrease in the size of the opening in the alumina mask during the vacuum deposition. The thicknesses of the Au and Al_2O_3 layers were 30 and 10 nm, respectively. These values were in good agreement with the nominal thickness of the layers in the vacuum deposition. The formation of the multilayer dots with a uniform thickness of Al_2O_3 could generate the 10 layers of accumulated gaps of 10 nm.

Fig. 3 shows the cross-sectional SEM images of multilayered nanodots with different numbers of Au layers, namely, 1, 3, and 5 layers. Even in this case, the size of the nanogaps between two Au layers could be controlled precisely in all samples.

The degree of enhancement of the electric field of incident light at the multilayered nanodot was simulated by 3D-FDTD method. Fig. 4 shows the result of the enhancement of the electric field of incident light around the multilayered nanodots. The numbers of Au layers were 3 in Fig. 4(a) and 5 in Fig. 4(b). The wavelength of the incident light was 633 nm considering the wavelength for the Raman measurements, and the polarization of the incident light was parallel to the *x*-direction. The strong enhancement of the electric field was observed at nanogaps between Au layers, reflecting the strong coupling of surface plasmon between Au layers. At the nanogap, the electric field was enhanced several tens times at almost every nanogap. This indicates that the increase of the number of layers in the nanodot can contribute to the formation of the substrates for effective SERS measurements.

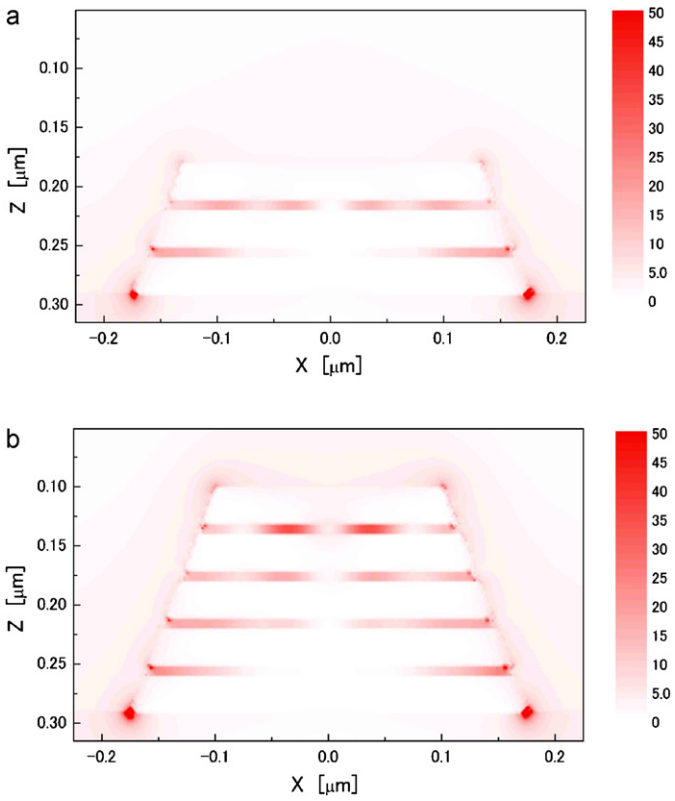

Fig. 4. Distributions of light intensity at the multilayered nanodot. The numbers of Au layers were (a) 3 and (b) 5. The incident light was a continuous wave of 633 nm.

By using the multilayered nanodot as the substrate for SERS measurement, it is expected that the SERS intensity can be increased with the number of layers compared with the single-layered nanodots. Fig. 5 shows the result of the Raman measurement of pyridine molecules adsorbed on the multilayered nanodots. For this measurement, multilayered nanodots with different numbers of gaps were used as a substrate. From the SERS spectra shown in Fig. 5(a), the enhancement of the Raman signals can be confirmed on the substrates with multilayered dots,

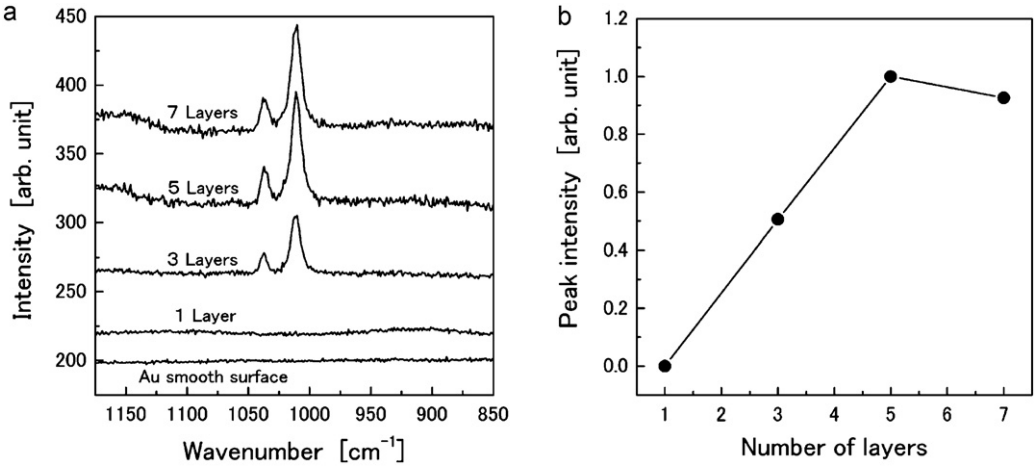

Fig. 5. (a) Raman spectra of pyridine molecules using multilayered nanodot arrays as substrates. The numbers of Au layers were 1, 3, 5 and 7. For comparison, an Au smooth surface was used for the measurement. (b) Dependence of SERS intensity on number of Au layers.

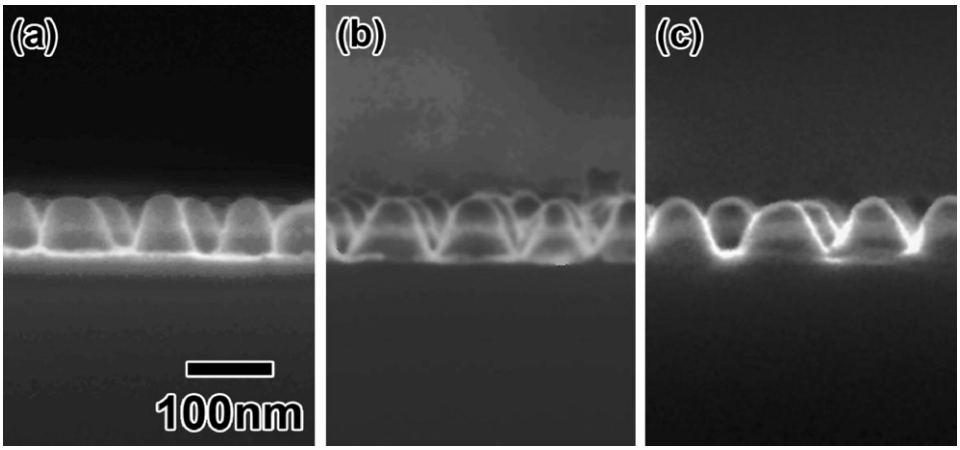

Fig. 6. SEM image of double-layered nanodots obtained by using self-ordered anodic porous alumina. The nanogap sizes were (a) 10 nm, (b) 15 nm, and (c) 20 nm. The diameter of the nanohole was 80 nm. The period of arrangement was 100 nm.

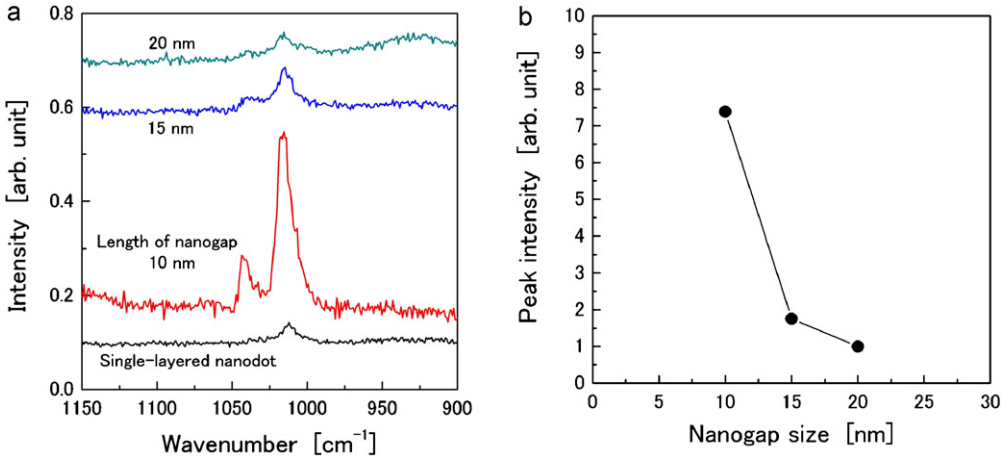

Fig. 7. (a) Raman spectra of pyridine molecules at double-layered nanodots. The lengths of nanogaps were 10, 15, and 20 nm. (b) Dependence of signal intensity on nanogap size between Au layers.

whereas no enhanced signals were observed in the case of smooth Au surface. The intensity of the SERS signals increased with number of layers owing to the increase in the number of sites for the effective enhancement of the electric field of incident light. In the enhanced Raman spectra, two clear peaks were observed at 1014 and 1040 cm^{-1}. These peaks originated from the molecular vibration, ring breathing, and trigonal ring breathing modes of pyridine molecules [19]. Fig. 5(b) summarizes the dependence of the intensity of the signals at the peaks at 1014 cm^{-1} on the number of Au layers. The intensity increased with the number of layers and almost saturated at 5 layers. The dependence of the intensity of the SERS signal on the number of layers was in good agreement with the simulated results obtained by the FDTD method.

Fig. 6 shows the SEM image of the multilayer dots with different nanogaps. In this case, the sizes of the nanogaps were controlled by changing the thickness of the Al_2O_3 layers between two Au layers from 10 to 20 nm.

Fig. 7 shows the dependence of the SERS signals on the size of the nanogap in the multilayered dots. Clear SERS spectra could be obtained in a smaller gap in the multilayered nanodots (Fig. 7(a)), and the intensity of the SERS signal (1014 cm^{-1}) was dependent on the size of gaps in the multilayered nanodots (Fig. 7(b)).

Fig. 8 shows the dependence of the degree of enhancement of electric fields of incident light on the size of the gap in the multilayered dots obtained by FDTD calculation. A higher electric field

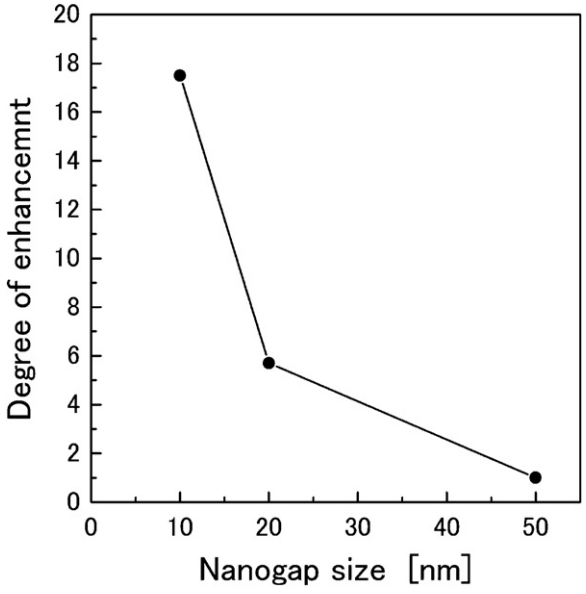

Fig. 8. Dependence of degree of enhancement of incident light on nanogap size.

was observed in a smaller gap between two Au layers. This result supports the experimental result showing the dependence of SERS the signal on the size of the nanogaps in the multilayered nanodots. From the results shown in Figs. 7 and 8, it can be concluded that the precise control of the size of the gap between two Au layers contributes to the effective enhancement of the electric field of incident light.

4. Conclusions

We demonstrated the fabrication of 3D multilayered nanodot composed of Au and Al_2O_3 using anodic porous alumina as a mask for vacuum deposition, and application to the substrate for SERS measurements. The accumulated nanogaps with controlled sizes were obtained on the basis of these structures, and the obtained nanogaps were confirmed to be useful for the effective enhancement of the electric fields of incident light. The multilayered nanodot array could be used as the substrate for the SERS measurement. The SERS signals were dependent on the geometrical structures of the multilayered nanodots; higher SERS signals were observed in the nanodots with a larger number of layers and a smaller size of gaps for the same number of layers.

This process is simple and applicable to the formation of multilayered nanodots composed of desired materials, and can be used for the fabrication of various types of functional plasmonic device, which can enhance the electric field of incident light effectively owing to its capability to precisely control 3D geometrical structures.

Acknowledgment

This work was partially supported by a Grant-in-Aid for Scientific Research No. 19049013 on the Priority Area “Strong Photons-Molecules Coupling Fields (470)” from the Ministry of Education, Culture, Sports, Science and Technology of Japan.

References

[1] S. Link, M.A. El-Sayed, J. Phys. Chem. B 103 (1990) 8410.
[2] L.J. Sherry, R. Jin, C.A. Mirkin, G.C. Schatz, R.P. Van Duyne, Nano Lett. 6 (2006) 2060.
[3] S. Zou, G.C. Schatz, Chem. Phys. Lett. 403 (2005) 62.
[4] T. Kondo, T. Fukushima, K. Nishio, H. Masuda, Appl. Phys. Express 2 (2009) 125001.
[5] T. Kondo, K. Nishio, H. Masuda, Appl. Phys. Express 2 (2009) 032001.
[6] T. Kondo, M. Tanji, K. Nishio, H. Masuda, Electrochem. Solid-State Lett. 9 (2006) C189.
[7] V. Malyarchuk, M.E. Stewart, R.G. Nuzzo, J.A. Rogers, Appl. Phys. Lett. 90 (2007) 203113.
[8] N. Yang, X. Su, V. Tjong, W. Knoll, Biosens. Bioelectron. 22 (2007) 2700.
[9] G.A. Wurtz, R. Pollard, A.V. Zayats, Phys. Rev. Lett. 97 (2006) 057402.
[10] K.H. Su, Q.H. Wei, X. Zhang, Appl. Phys. Lett. 88 (2006) 063118.
[11] N. Murazawa, D. Aoyou, K. Ueno, V. Mizeikis, S. Juodkazis, H. Misawa, Annual Meeting on Photochemistry 1A 17, 2009.
[12] H. Masuda, M. Satoh, Jpn. J. Appl. Phys. 35 (1996) L126.
[13] H. Masuda, K. Yasui, K. Nishio, Adv. Matter. 12 (2000) 1031.
[14] K. Yasui, Y. Sakamoto, K. Nishio, H. Masuda, Chem. Lett. 34 (2005) 342.
[15] M. Harada, T. Kondo, T. Yanagishita, K. Nishio, H. Masuda, Appl. Phys. Express 3 (2010) 015001.
[16] F. Matsumoto, M. Ishikawa, K. Nishio, H. Masuda, Chem. Lett. 34 (2005) 508.
[17] T. Kondo, F. Matsumoto, K. Nishio, H. Masuda, Chem. Lett. 37 (2008) 466.
[18] H. Masuda, K. Fukuda, Science 268 (1995) 1466.
[19] D.Y. Wu, M. Hayashi, S.H. Lin, Z.Q. Tian, Spectrochim. Acta Part A 60 (2004) 137.